J|A|C|S
ARTICLES

Published on Web 12/30/2008

Protein Cold Denaturation as Seen From the Solvent

Monika Davidovic, Carlos Mattea,† Johan Qvist, and Bertil Halle*

Department of Biophysical Chemistry, Center for Molecular Protein Science, Lund University, SE-22100 Lund, Sweden

Received July 19, 2008

Abstract: Unlike most ordered molecular systems, globular proteins exhibit a temperature of maximum stability, implying that the structure can be disrupted by cooling. This cold denaturation phenomenon is usually linked to the temperature-dependent hydrophobic driving force for protein folding. Yet, despite the key role played by protein−water interactions, hydration changes during cold denaturation have not been investigated experimentally. Here, we use water−^{17}O spin relaxation to monitor the hydration dynamics of the proteins BPTI, ubiquitin, apomyoglobin, and β-lactoglobulin in aqueous solution from room temperature down to −35 °C. To access this temperature range without ice formation, we contained the protein solution in nonperturbing picoliter emulsion droplets. Among the four proteins, only the destabilized apomyoglobin was observed to cold denature. Ubiquitin was found to be thermodynamically stable at least down to −32 °C, whereas β-lactoglobulin is expected to be unstable below −5 °C but remains kinetically trapped in the native state. When destabilized by 4 M urea, β-lactoglobulin cold denatures at 10 °C, as found previously by other methods. As seen from the solvent, the cold-denatured states of apomyoglobin in water and β-lactoglobulin in 4 M urea are relatively compact and are better described as solvent-penetrated than as unfolded. This finding challenges the popular analogy between cold denaturation and the anomalous low-temperature increase in aqueous solubility of nonpolar molecules. Our results also suggest that the reported cold denaturation at −20 °C of ubiquitin encapsulated in reverse micelles is caused by the low water content rather than by the low temperature.

1. Introduction

Under physiological conditions, most natural polypeptides adopt a unique, biologically active conformation. The high cooperativity of this folding process greatly simplifies the analysis of protein stability, allowing many single-domain proteins to be described in terms of a two-state equilibrium between a native (N) and a denatured (D) state.[1,2] Ordered molecular systems are usually more stable at low temperatures, where thermal fluctuations are suppressed, but native proteins tend to be most stable at a temperature, T^*, near room temperature.[3−5] As a consequence, the D-state population can be increased either by heating (for $T > T^*$) or by cooling (for $T < T^*$). At sufficiently high or low temperatures, the native protein is thus denatured, meaning that the D state is more populated than the N state. These two ways of disrupting the native protein conformation are known as heat denaturation and cold denaturation, respectively.[6]

The term cold denaturation usually refers to the *process* whereby a protein is denatured by reducing the temperature. However, equilibrium thermodynamics deals with *states*, and the properties of a particular cold-denatured state must be independent of the path by which it was reached. According to the standard two-state model, there is only one D state with continuously (noncooperatively) variable properties. The D state can be said to be cold-denatured whenever it has lower enthalpy than the N state, so that its population increases on cooling. Cold denaturation is phenomenologically linked to the large increase of the isobaric heat capacity on denaturation, responsible for the dome-shaped free-energy function, $\Delta G(T) = G_D(T) - G_N(T)$.[5−7] While still somewhat controversial,[8] the large ΔC_p has long been attributed principally to the hydration of nonpolar side-chains that become solvent-exposed upon disruption of the protein's hydrophobic core.[9−11] In the conventional view, there is thus a close analogy between cold denaturation of proteins and cold swelling of hydrophobic polymers or the anomalous low-temperature enhancement of the solubility of nonpolar organic solutes in water.[12,13] Statistical−mechanical studies of the cold-denaturation mechanism are generally based on this assumption.[14−22]

† Present address: Institute of Physics, Technical University of Ilmenau, D-98684 Ilmenau, Germany.

(1) Kauzmann, W. *Adv. Protein Chem.* **1959**, *14*, 1–63.
(2) *Protein Folding Handbook*; Buchner, J., Kiefhaber, T., Eds.; Wiley-VCH: Weinheim, 2005.
(3) Brandts, J. F. *J. Am. Chem. Soc.* **1964**, *86*, 4291–4301.
(4) Hawley, S. A. *Biochemistry* **1971**, *10*, 2436–2442.
(5) Kumar, S.; Tsai, C.-J.; Nussinov, R. *Biochemistry* **2002**, *41*, 5359–5374.
(6) Privalov, P. L. *Crit. Rev. Biochem. Mol. Biol.* **1990**, *25*, 281–305.
(7) Makhatadze, G. I. *Biophys. Chem.* **1998**, *71*, 133–156.
(8) Prabhu, N. V.; Sharp, K. A. *Annu. Rev. Phys. Chem.* **2005**, *56*, 521–548.
(9) Baldwin, R. L. *Proc. Natl. Acad. Sci. U.S.A.* **1986**, *83*, 8069–8072.
(10) Dill, K. A. *Biochemistry* **1990**, *29*, 7133–7155.
(11) Makhatadze, G. I. In *Protein Folding Handbook*; Buchner, J., Kiefhaber, T., Eds.; Wiley-VCH: Weinheim, 2005; Vol. I, pp 70−98.
(12) Blokzijl, W.; Engberts, J. B. F. N. *Angew. Chem., Int. Ed.* **1993**, *32*, 1545–1579.
(13) Southall, N. T.; Dill, K. A.; Haymet, A. D. J. *J. Phys. Chem. B* **2002**, *106*, 521–533.

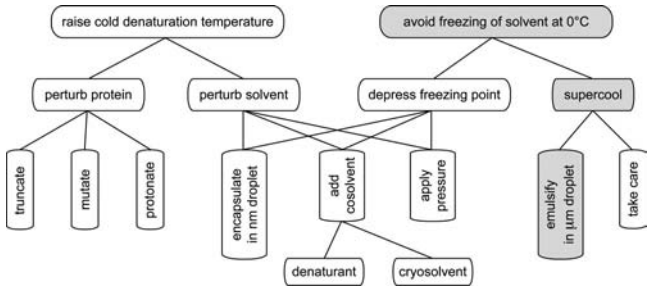

Figure 1. Different experimental strategies for observing cold denaturation. The degree of perturbation of the protein−solvent system decreases roughly from left to right in this chart. The approach used here is indicated by the shaded boxes.

For a two-state protein, the cold-denaturation temperature, T_{cd}, can be estimated by extrapolating the thermodynamic parameters that characterize heat denaturation.[3−5] The predicted T_{cd} is typically 20 K or more below the equilibrium freezing point of water. To observe cold denaturation, it is thus necessary to raise T_{cd} (by destabilizing N or stabilizing D) and/or to prevent the solvent from freezing (Figure 1). To date, most cold-denaturation studies have employed modified proteins, non-physiological solvents, or high pressure. In the earliest studies of cold-denatured proteins, the D state was stabilized by urea,[23−26] which, along with guanidinium chloride, remains the most popular strategy for making cold denaturation experimentally accessible.[27−36] More recently, application of hydrostatic pressure has been used to raise T_{cd}.[37−43] Cosolvents and elevated pressure both have the additional desirable effect of depressing the equilibrium freezing point of the solvent.

To understand the role of (hydrophobic) hydration for the stability and folding of proteins under physiological conditions, we need to study proteins in their natural aqueous environment, unperturbed by cosolvents, high pressure, or confinement/dehydration. Cold denaturation without solvent perturbations has been studied with proteins destabilized by charge perturbations (usually at reduced pH), amino acid replacements, or truncation of the polypeptide chain.[44−55]

If the solvent water can be maintained in a supercooled state, a wider temperature range becomes available for cold-denaturation studies. Using capillaries[54] or specially designed sample cells,[51] temperatures down to −20 °C have been reached. By subdividing the protein solution into picoliter droplets suspended in an inert nonpolar carrier fluid in a water-in-oil emulsion, protein solutions can be studied at least down to −35 °C, where the rate of homogeneous ice nucleation becomes the limiting factor.[56−58] Emulsion samples interfere with most scattering and optical spectroscopic measurements, but they were used early on to study cold denaturation at subzero temperatures via UV absorbance.[44,59] Here, we use the emulsion approach and NMR relaxation measurements to detect cold denaturation and to characterize the hydration of the cold-denatured state in aqueous protein solutions down to −35 °C.

Cold denaturation is often taken as evidence for hydrophobic stabilization of native proteins. Yet, to our knowledge, the hydration of cold-denatured proteins has not been studied. As one of few techniques that can selectively monitor the water molecules in a protein solution, water−^{17}O magnetic relaxation dispersion (MRD) has been used to characterize the single-molecule water dynamics in the hydration layer of native[60,61] and non-native[62] proteins. ^{17}O MRD studies have thus been

(14) Hansen, A.; Jensen, M. H.; Sneppen, K.; Zocchi, G. *Eur. Phys. J. B* **1998**, *6*, 157–161.
(15) Robinson, G. W.; Cho, C. H. *Biophys. J.* **1999**, *77*, 3311–3318.
(16) De Los Rios, P.; Caldarelli, G. *Phys. Rev. E* **2001**, *63*, 031802.
(17) Tsai, C.-J.; Maizel, J. V.; Nussinov, R. *Crit. Rev. Biochem. Mol. Biol.* **2002**, *37*, 55–69.
(18) Bakk, A.; Høye, J. S.; Hansen, A. *Biophys. J.* **2002**, *82*, 713–719.
(19) Marqués, M. I.; Borreguero, J. M.; Stanley, H. E.; Dokholyan, N. V. *Phys. Rev. Lett.* **2003**, *91*, 138103.
(20) Paschek, D.; Nonn, S.; Geiger, A. *Phys. Chem. Chem. Phys.* **2005**, *7*, 2780–2786.
(21) Patel, B. A.; Debenedetti, P. G.; Stillinger, F. H.; Rossky, P. J. *Biophys. J.* **2007**, *93*, 4116–4127.
(22) Lopez, C. F.; Darst, R. K.; Rossky, P. J. *J. Phys. Chem. B* **2008**, *112*, 5961–5967.
(23) Hopkins, F. G. *Nature* **1930**, *126*, 383–384.
(24) Jacobsen, C. F.; Christensen, L. K. *Nature* **1948**, *161*, 30–31.
(25) Schellman, J. A. *Compt. rend. Lab. Carlsberg, Sér. chim.* **1958**, *30*, 395–414.
(26) Pace, N. C.; Tanford, C. *Biochemistry* **1968**, *7*, 198–208.
(27) Chen, B.-L.; Schellman, J. A. *Biochemistry* **1989**, *28*, 685–691.
(28) Griko, Y. V.; Venyaminov, S. Y.; Privalov, P. L. *FEBS Lett.* **1989**, *244*, 276–278.
(29) Griko, Y. V.; Privalov, P. L. *Biochemistry* **1992**, *31*, 8810–8815.
(30) Griko, Y. V.; Kutyshenko, V. P. *Biophys. J.* **1994**, *67*, 356–363.
(31) Agashe, V. R.; Udgaonkar, J. B. *Biochemistry* **1995**, *34*, 3286–3299.
(32) Huang, G. S.; Oas, T. G. *Biochemistry* **1996**, *35*, 6173–6180.
(33) Ibarra-Molero, B.; Makhatadze, G. I.; Sanchez-Ruiz, J. M. *Biochim. Biophys. Acta* **1999**, *1429*, 384–390.
(34) Mizuguchi, M.; Hashimoto, D.; Sakurai, M.; Nitta, K. *Proteins* **2000**, *38*, 407–413.
(35) Katou, H.; Hoshino, M.; Kamikubo, H.; Batt, C. A.; Goto, Y. *J. Mol. Biol.* **2001**, *310*, 471–484.
(36) Tang, X.; Pikal, M. J. *Pharm. Res.* **2005**, *22*, 1167–1175.
(37) Zhang, J.; Peng, X.; Jonas, A.; Jonas, J. *Biochemistry* **1995**, *34*, 8631–8641.
(38) Nash, D. P.; Jonas, J. *Biochemistry* **1997**, *36*, 14375–14383.
(39) Nash, D. P.; Jonas, J. *Biochem. Biophys. Res. Commun.* **1997**, *238*, 289–291.
(40) Valente-Mesquita, V. L.; Botelho, M. M.; Ferreira, S. T. *Biophys. J.* **1998**, *75*, 471–476.
(41) Jonas, J.; Ballard, L.; Nash, D. *Biophys. J.* **1998**, *75*, 445–452.
(42) Kunugi, S.; Tanaka, N. *Biochim. Biophys. Acta* **2002**, *1595*, 329–344.
(43) Kitahara, R.; Okuno, A.; Kato, M.; Taniguchi, Y.; Yokoyama, S.; Akasaka, K. *Magn. Reson. Chem.* **2006**, *44*, S108–S113.
(44) Franks, F.; Hatley, R. H. M. *Cryo-Lett.* **1985**, *6*, 171–180.
(45) Privalov, P. L.; Griko, Y. V.; Venyaminov, S. Y.; Kutyshenko, V. P. *J. Mol. Biol.* **1986**, *190*, 487–498.
(46) Griko, Y. V.; Privalov, P. L.; Sturtevant, J. M.; Venyaminov, S. Y. *Proc. Natl. Acad. Sci. U.S.A.* **1988**, *85*, 3343–3347.
(47) Griko, Y. V.; Privalov, P. L.; Venyaminov, S. Y.; Kutyshenko, V. P. *J. Mol. Biol.* **1988**, *202*, 127–138.
(48) Tamura, A.; Kimura, K.; Takahara, H.; Akasaka, K. *Biochemistry* **1991**, *30*, 11307–11313.
(49) Nishii, I.; Kataoka, M.; Tokunaga, F.; Goto, Y. *Biochemistry* **1994**, *33*, 4903–4909.
(50) Konno, T.; Kataoka, M.; Kamatari, Y.; Kanaori, K.; Nosaka, A.; Akasaka, K. *J. Mol. Biol.* **1995**, *251*, 95–103.
(51) Sabelko, J.; Ervin, J.; Gruebele, M. *J. Phys. Chem. B* **1998**, *102*, 1806–1819.
(52) Richardson, J. M.; Lemaire, S. D.; Jacquot, J.-P.; Makhatadze, G. I. *Biochemistry* **2000**, *39*, 11154–11162.
(53) Pastore, A.; Martin, S. R.; Politou, A.; Kondapalli, K. C.; Stemmler, T.; Temussi, P. A. *J. Am. Chem. Soc.* **2007**, *129*, 5374–5375.
(54) Szyperski, T.; Mills, J. L.; Perl, D.; Balbach, J. *Eur. Biophys. J.* **2006**, *35*, 363–366.
(55) Li, Y.; Shan, B.; Raleigh, D. P. *J. Mol. Biol.* **2007**, *368*, 256–262.
(56) Rasmussen, D. H.; MacKenzie, A. P. *J. Chem. Phys.* **1973**, *59*, 5003–5013.
(57) Douzou, P.; Debey, P.; Franks, F. *Biochim. Biophys. Acta* **1978**, *523*, 1–8.
(58) Franks, F. *Adv. Protein Chem.* **1995**, *46*, 105–139.
(59) Hatley, R. H. M.; Franks, F. *FEBS Lett.* **1989**, *257*, 171–173.
(60) Halle, B. *Phil. Trans. R. Soc. Lond. B* **2004**, *359*, 1207–1224.
(61) Mattea, C.; Qvist, J.; Halle, B. *Biophys. J.* **2008**, *95*, 2951–2963.
(62) Halle, B.; Denisov, V. P.; Modig, K.; Davidovic, M. In *Protein Folding Handbook*; Buchner, J., Kiefhaber, T., Eds.; Wiley-VCH: Weinheim, 2005; Vol. I, pp 201−246.

Table 1. Results Derived from Fits to ^{17}O MRD Data[a]

protein	solvent	pH	# data	ν_N	ν_D	E_{HN}^{-} (kJ mol^{-1})	E_{HD} (kJ mol^{-1})	N_{HD}/N_{HN}	T_{cd}(°C)	ΔT_{cd}(°C)
BPTI	water	5.2	8	2.31(1)		26.4(4)				
mUb	water	5.0	14	2.32(1)		27.2(2)				
aMb	water	5.8	41	2.06(1)	1.72(1)	[27]	[27]	0.88(3)	−16(1)	14(2)
bLg	water	2.6	39	2.17(1)		27.6(4)				
bLg	4 M urea	2.6	47	2.07(2)	2.21(3)	[27.6]	34(1)	1.3(1)	10.0(3)	[10]
bLg	4 M urea	2.6	23[b]	2.09(2)	2.13(7)	[27.6]	25(4)	1.4(3)	11.0(7)	[10]
bLg	water	7.2	82	2.01(1)	1.56(5)	[27.6]	[27.6]	0.9(2)	−36(7)	30(4)

[a] Uncertainty in last digit given within parentheses. Parameter values within square brackets were frozen in the fit. [b] Fit to restricted data set, consisting of MRD profiles at 19.4, 10.2, and −1.1 °C.

reported of proteins denatured by urea,[63] guanidinium chloride,[64] low pH,[64] and heat.[65] Here, we describe the first ^{17}O MRD study of cold-denatured proteins. We have investigated four proteins that are popular model systems for protein folding studies: bovine pancreatic trypsin inhibitor (BPTI), mammalian ubiquitin (mUb), equine apomyoglobin (aMb), and bovine β-lactoglobulin (bLg). The first two of these proteins do not cold denature under the conditions examined here and therefore serve as models for native proteins at low temperatures.[61]

2. Materials and Methods

2.1. Sample Preparation. Bovine pancreatic trypsin inhibitor (BPTI, batch 9104, 97% purity by HPLC) from Bayer HealthCare AG (Wuppertal, Germany) was exhaustively dialyzed to remove residual salt. Mammalian ubiquitin (mUb) was expressed in *Escherichia coli* and was purified to >99% as described.[66] Apomyoglobin (aMb) was prepared from equine myoglobin (Sigma, M-0630, > 95% purity) by heme extraction with 2-butanone at pH 2,[67] followed by exhaustive dialysis at 8 °C. The residual absorbance in the 409 nm Soret band indicated <1% heme occupancy. Bovine β-lactoglobulin (bLg) isoform A (Sigma, L-7880) was purified by anion exchange and size-exclusion chromatography, followed by dialysis.[68] Protein solutions were prepared by dissolving the purified lyophilized protein in ^{17}O-enriched (20−40 atom % ^{17}O, Isotec) H_2O or (to allow ^{2}H MRD control measurements) a mixture of ^{17}O-enriched H_2O and D_2O (99.9 atom % ^{2}H, low paramagnetic content, CIL). The bLg samples at neutral pH also contained 0.02% sodium azide. After adjusting pH to the desired value, the solution was centrifuged to remove any aggregates. A small fraction of each MRD sample was subjected to complete amino acid analysis to determine the protein concentration with ∼1% accuracy. The ^{17}O relaxation enhancement produced by the protein is inversely proportional to the water/protein mole ratio N_W, which can be calculated from the protein concentration. The bLg solutions in 4 M urea were prepared by adding the required mass of dry urea (>99%, pro analysi grade, Merck) to the aqueous protein solution. pH was measured at room temperature and is quoted without H/D isotope correction.

Relaxation measurements at temperatures below the equilibrium freezing point of the solvent were performed on emulsion samples,[56] prepared by mixing ∼1 mL protein solution with an equal volume of *n*-heptane (>99%, HPLC grade, Sigma) containing 3% (w/w) of the nonionic emulsifier sorbitan tristearate (Sigma). A sufficiently stable water-in-oil emulsion was obtained by mixing the two solutions with the aid of two 5 mL syringes connected via a 0.56 mm i.d. nozzle (Hamilton) and pressing the mixture through the nozzle ∼40 times. In a typical aqueous droplet of 10 μm diameter, only 0.3% of the protein molecules in the solution are within 5 nm of the interface. Furthermore, polyols (like the sorbitan headgroup of the emulsifier) are preferentially excluded from protein surfaces,[69] so the protein should not interact strongly with the interface. Indeed, no effect of the interface could be detected in control experiments where ^{17}O MRD profiles were recorded (at room temperature) from the same protein solution before and after incorporation in emulsion droplets (part a of Figure 3 and part a of Figure 6). Relevant sample characteristics are summarized in Table S1 of the Supporting Information.

2.2. Spin Relaxation Measurements. The relaxation rate, R_1, of the water−^{17}O longitudinal magnetization was measured either as a function of temperature, T, at a fixed ^{17}O resonance frequency, ν_0 = 81.3 MHz (corresponding to 600 MHz ^{1}H frequency), or as a function of resonance frequency at a fixed temperature. The results of these two types of measurement series will be referred to as temperature profiles and MRD profiles, respectively. R_1 was determined from a three-parameter fit to the single-exponential magnetization curve obtained with the inversion recovery pulse sequence with 20 delay times in nonmonotonic order and a sufficient number of transients to obtain a signal-to-noise ratio of >100. Acoustic ringing, which interferes at low fields (<0.3 T) and low temperatures (where T_1 is short), was suppressed using filters or a modified 90° pulse[70] in the inversion recovery sequence. The ice signal from the small fraction of frozen water droplets is broadened beyond detection and does not affect the R_1 measurement. The small scatter in the inversion recovery fits indicates that freezing does not occur to a significant extent during relaxation measurements at subzero temperatures. This was the case even at the lowest temperature (−35 °C) accessed here.

Most of the ^{17}O MRD profiles reported here extend from 0.57 or 2.2 MHz up to 67.8 or 81.3 MHz. Frequencies <11 MHz were accessed with field-variable iron-core magnets (Drusch EAR-35N or GMW 3474−140) interfaced to Tecmag (Apollo or Discovery) consoles, whereas higher frequencies were provided by conventional superconducting magnets interfaced to commercial NMR spectrometers (Bruker Avance DMX 100 and 200, Varian Unity Plus 360, 500 and 600). At each temperature and frequency, we also measured the relaxation rate, R_1^0, of a reference sample containing the solvent present in the corresponding protein solution. All samples were equilibrated at the measurement temperature (see sect. 4.5), which was regulated with a precooled stream of dry air and determined before and after R_1 measurements with a copper-constantan thermocouple in an NMR tube containing a water−ethanol mixture. Sample temperature variations during R_1 measurements were <0.1 K for the superconducting magnets, increasing to 0.2−0.3 K for the iron-core magnets at the lowest temperatures. On the basis of the scatter in the frequency-independent R_1^0, the accuracy in R_1 ranged from <0.5% in temperature profiles to 1−2% in low-temperature MRD profiles. Data matrices $R_1(\omega_0,T)$ comprising 39−82 R_1 values from several MRD profiles and one T profile

(63) Modig, K.; Kurian, E.; Prendergast, F. G.; Halle, B. *Protein Sci.* **2003**, *12*, 2768–2781.
(64) Denisov, V. P.; Jonsson, B.-H.; Halle, B. *Nat. Struct. Biol.* **1999**, *6*, 253–260.
(65) Denisov, V. P.; Halle, B. *Biochemistry* **1998**, *37*, 9595–9604.
(66) Persson, E.; Halle, B. *J. Am. Chem. Soc.* **2008**, *130*, 1774–1787.
(67) Teale, F. W. J. *Biochim. Biophys. Acta* **1959**, *35*, 543.
(68) Qvist, J.; Davidovic, M.; Hamelberg, D.; Halle, B. *Proc. Natl. Acad. Sci. U.S.A.* **2008**, *105*, 6296–6301.
(69) Timasheff, S. N. *Biochemistry* **2002**, *41*, 13473–13482.
(70) Patt, S. L. *J. Magn. Reson.* **1982**, *49*, 161–163.

were analyzed by global fits using the Marquardt−Levenberg nonlinear least-squares algorithm.

3. Results

3.1. Protein Hydration from Water ^{17}O MRD Data. The dependence of the water−^{17}O spin relaxation rate, $R_1(\omega_0,T)$, on resonance frequency, ω_0, and temperature, T, provides information about the number of water molecules that interact directly with the protein and about their rotational correlation times. In a protein solution, $R_1(\omega_0,T)$ exceeds the relaxation rate, R_1^0, for the bulk solvent because water molecules that interact with the protein rotate more slowly. The dynamically perturbed water molecules can be divided in two classes. A small number, N_I, of *internal* water molecules are buried in cavities with residence time $\tau_I > \sim 10$ ns at room temperature. A much larger number, N_H, of more mobile water molecules interact with the external surface of the protein, constituting the *hydration layer*. The hydration number N_H can be estimated by dividing the solvent-accessible surface area of the protein with the effective surface area, 10.75 Å^2, occupied by one water molecule. For proteins[61] as well as for peptides and small organic solutes,[71] this simple procedure yields N_H values in excellent agreement with results from MD simulations with cutoff distances based on radial distribution functions.

We present the relaxation data in the form of an apparent dynamic perturbation factor (ADPF), defined as

$$\xi(\omega_0,T) \equiv 1 + \frac{N_W}{N_{HN}}\left[\frac{R_1(\omega_0,T) - R_1^0(T)}{R_1^0(T)}\right] \quad (1)$$

The ADPF is obtained directly from the measured quantities $R_1(\omega_0,T)$, $R_1^0(T)$, and N_W (the water/protein mole ratio in the sample) and the hydration number N_{HN} calculated from the known structure of the native protein (Table S1 of the Supporting Information). By normalizing the R_1 data in this way, we remove the effect of protein concentration and most of the effects of protein size and solvent composition. Furthermore, in the limit $\omega_0 = 0$ (or when all correlation times are short compared to $1/\omega_0$), the ADPF reduces to the *true* (rather than apparent) DPF, $\xi(T) \equiv \langle\tau\rangle/\tau_0$, which relates hydration-water dynamics to bulk-water dynamics in an essentially model- and method-independent way.[61]

For a native protein (i.e., in the absence of cold denaturation), the ADPF is a sum of two contributions (section S1 of the Supporting Information). The internal-water contribution (colored red in the following figures) is negligibly small at low temperatures or high frequencies. Under conditions where the internal-water contribution is non-negligible, it can be accurately estimated from the known protein tumbling time and the residence time and order parameter of the internal water molecules (section S2 of the Supporting Information). The ADPF is usually dominated by the contribution (colored blue in the following figures) from the N_{HN} water molecules in the hydration layer. The rotational correlation times of these water molecules range from picoseconds to nanoseconds (at room temperature) and can be modeled by a power-law distribution[61] (section S1 of the Supporting Information). The two parameters in this model, the power-law exponent, ν_N, and the activation energy, E_{HN}^-, of water rotation at the short-correlation-time end of the distribution, can be determined from a fit to a temperature profile $R_1(\omega_0,T)$ at a fixed high frequency and extending to sufficiently low temperatures (in the supercooled regime).[61]

The extension of the model to the case of coexisting native (N) and denatured (D) protein molecules in the solution is straightforward (section S1 of the Supporting Information). The ADPF now contains a third contribution (colored yellow in the following figures), associated with the N_{HD} water molecules that are in contact with the denatured protein. At temperatures where the protein is fully denatured, the model contains three parameters: N_{HD}, ν_D, and E_{HD}^-. To analyze ^{17}O relaxation data at temperatures where the N and D forms coexist, we model their relative populations in terms of two parameters: the cold denaturation temperature, T_{cd}, and the transition width, ΔT_{cd} (section S1 of the Supporting Information). To determine the model parameters, we perform global fits to large sets of $R_1(\omega_0,T)$ data, comprising a temperature profile (extending far into the supercooled regime) at a high fixed frequency as well as two or more dispersion profiles at fixed temperatures. In most cases, the number of free parameters can be reduced by physically motivated approximations (see below).

3.2. BPTI. At the temperatures examined here (down to −35 °C), BPTI is expected to remain fully folded (Discussion). The temperature-dependent water−^{17}O relaxation data for BPTI (part a of Figure 2) thus serve as a baseline for the more complex situations encountered with proteins that do cold denature. The internal-water contribution to the ADPF (section S2 of the Supporting Information) is negligibly small at low temperatures, where the protein tumbling rate is much smaller than the high ^{17}O resonance frequency (81.3 MHz) of these measurements.

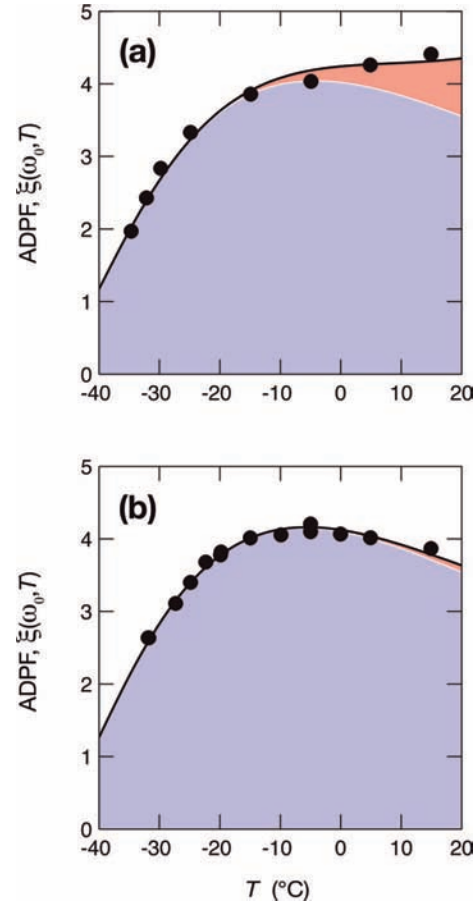

Figure 2. Temperature dependence of the water−^{17}O ADPF at 81.3 MHz for (a) BPTI (sample 1) and (b) mUb (sample 2). The curves were obtained by fitting the two model parameters ν_N and E_{HN}^- (Table 1) to the data (filled circles). The computed ADPF contributions from internal water (red) and hydration water (blue) are indicated.

(71) Qvist, J.; Halle, B. *J. Am. Chem. Soc.* **2008**, *130*, 10345–10353.

The hydration-layer contribution to the ADPF exhibits a broad maximum near −5 °C, where $\xi(\omega_0,T) \approx 4$. As discussed in detail elsewhere,[61] this maximum reflects a crossover of the (temperature-dependent) activation energies of water rotation in the hydration layer and in the bulk solvent, with the latter having the largest activation energy at low temperatures. The true hydration-layer DPF, $\xi_H(T)$, which can be calculated[61] from the parameters ν_N and E_{HN}^- (Table 1), exhibits a similar maximum near −10 °C, where $\xi_H \approx 4.8$. Because the distribution of correlation times in the hydration layer is very broad, slow hydration water molecules (say, with $\tau_H > 0.1$ ns at 20 °C) contribute significantly to the DPF even though they are few in number (0.5%). Accordingly, the maximum DPF for the 90 or 50% most mobile hydration water molecules drops to 2.4 and 1.6, respectively. These partial DPF values represent the dominant generic part of the hydration layer and are similar to the DPF values obtained for small peptides and other organic solutes.[71]

3.3. Ubiquitin. On the basis of previous work (Discussion), we expect T_{cd} to be around −50 °C (at pH 5.0) so that cold denaturation of mUb should not occur in our temperature range. This prediction is confirmed by the very similar temperature profiles that we observe for mUb and BPTI (Figure 2). The slightly larger ADPF for BPTI at the highest temperatures is fully accounted for by the larger internal-water contribution for BPTI (section S2 of the Supporting Information). The fits to the data in Figure 2 show that the hydration dynamics parameters ν_N and E_{HN}^- are virtually identical for mUb and BPTI (Table 1), as expected if both proteins remain fully folded at all investigated temperatures. We therefore conclude that mUb remains fully folded at least down to −32 °C.

3.4. Apomyoglobin. Removal of the heme group causes partial unfolding of myoglobin, with a 20% reduction in α-helix content.[49] The consequent stability reduction has allowed cold denaturation of aMb to be observed (by far-UV circular dichroism) not far below 0 °C.[49,51] The temperature profile of aMb (part c of Figure 3) does indeed differ qualitatively from those of BPTI and mUb (Figure 2), but these data alone do not contain sufficient information to determine the additional model parameters associated with the cold-denatured (D) state. We therefore acquired MRD profiles at 27 °C, where aMb is fully native (part a of Figure 3), and at −20 °C, where the ADPF is dominated by the D state (part b of Figure 3). At 27 °C, measurements were performed directly on the aMb solution as well as on the emulsion sample made from the same solution. As seen from part a of Figure 3, incorporation of the protein solution into micrometer-sized emulsion droplets has no significant effect on the measured ^{17}O relaxation. The negligible influence of the droplet interface has previously been demonstrated also for BPTI.[72] In the global fit to the 41 data points in Figure 3, we constrained E_{HN}^- to the same value (27 kJ mol^{-1}) as found for BPTI and mUb (Table 1). This parameter describes the most mobile part of the hydration layer, which should be similar for all globular proteins.[61] For the same reason, we expect E_{HD}^- to be similar to E_{HN}^-. Accordingly, we imposed the constraint $E_{HD}^- = E_{HN}^-$.

The N-state exponent obtained from the global fit, $\nu_N = 2.06$, is slightly smaller than for BPTI and mUb, corresponding to a somewhat wider distribution of correlation times, that is, a larger proportion of relatively long correlation times. This feature may be associated with the large solvent-filled heme cavity and the disordered F helix in aMb.[73] The D state has an even broader distribution, with $\nu_D = 1.72$, as expected if the cold-denatured protein is penetrated by water. To illustrate the significance of these power-law exponents, we can calculate the fraction of hydration water molecules with correlation times τ_H longer than, say, 0.1 ns at 20 °C.[61] This fraction is 1.5% for the N state and 5.6% for the D state of aMb (and 0.5% for BPTI and mUb).

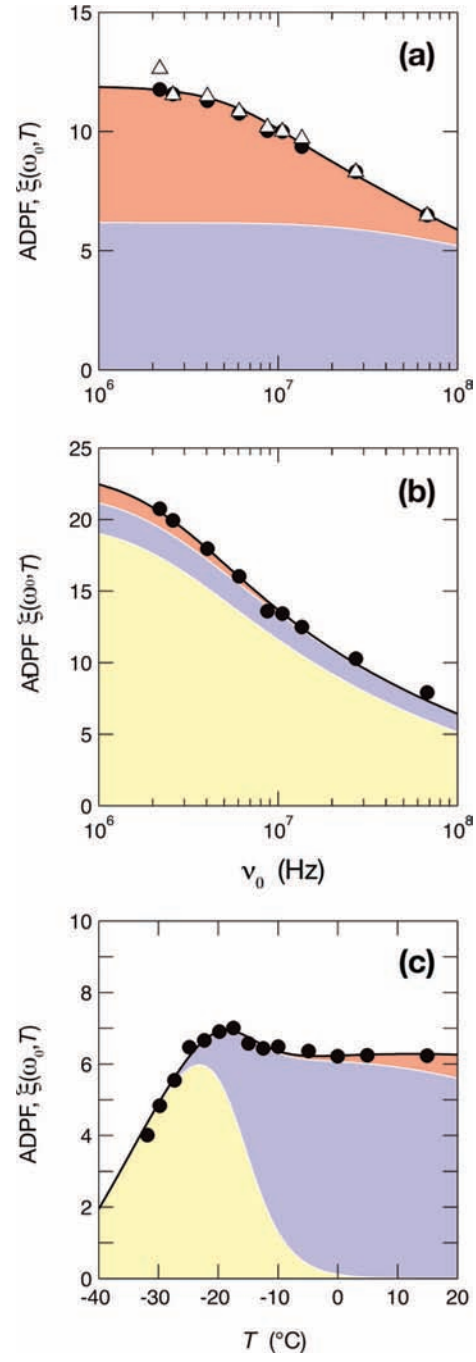

Figure 3. Variation of the water−^{17}O ADPF for aMb at pH 5.8 with frequency (sample 3) at (a) 27 °C, (b) −20 °C, and (c) with temperature (sample 4) at 81.3 MHz. The solid curves were obtained from a global fit to all data (filled circles, emulsion; open triangles, solution). The resulting parameter values are given in Table 1. The computed ADPF contributions from internal water (red) and N-state (blue) or D-state (yellow) hydration water are indicated.

(72) Jóhannesson, H.; Halle, B. *J. Am. Chem. Soc.* **1998**, *120*, 6859–6870.

(73) Eliezer, D.; Wright, P. E. *J. Mol. Biol.* **1996**, *263*, 531–538.

For the cold-denaturation transition, the fit yields $T_{cd} = -16 \pm 1$ °C and $\Delta T_{cd} = 14 \pm 2$ °C. Cold denaturation is expected to increase the solvent-accessible area and thereby the number of water molecules in contact with the protein. However, our analysis indicates that this number actually *decreases*: $N_{HD}/N_{HN} = 0.88 \pm 0.03$. To rationalize this unexpected result, we recall that aMb has an exceptionally low packing density: disordered and relatively mobile water molecules are expected to penetrate the large heme cavity and at least some of the several smaller cavities. Presumably, cold denaturation causes these cavities to collapse, thus effectively reducing the solvent-exposed surface area of the protein. At the same time, other water molecules penetrate the structurally disordered protein. Although cold denaturation reduces the total solvent exposure slightly, it increases the number of strongly perturbed water molecules. With $N_{HN} = 719$ (Table S1 of the Supporting Information), we can thus infer that the number of water molecules with $\tau_H > 0.1$ ns (at 20 °C) increases from 11 in the N state to 35 in the D state.

3.5. β-Lactoglobulin at pH 2.6. Bovine β-lactoglobulin is predominantly dimeric at neutral pH, but at pH 2.6 and in salt-free solvent, as in samples 5−9 (Table S1 of the Supporting Information), the dimer fraction is <10%.[74] The dimer interface buries only 6% of the solvent-accessible area[75] (with a correspondingly small reduction of N_{HN}; Table S1 of the Supporting Information) so a few percent dimer should not significantly affect the water−^{17}O ADPF.

The global fit comprises 39 data points, including a temperature profile (part d of Figure 4), MRD profiles at 19.4, 10.2, and −1.1 °C (parts a−c of Figure 4) and partial MRD profiles at −20 and −25 °C (Table S1 of the Supporting Information). The data, extending down to −35 °C, show no sign of cold denaturation. The hydration parameters, $\nu_N = 2.17$ and $E_{HN}^{-} = 27.6$ kJ mol^{-1}, do not differ significantly from what was obtained from a previous fit to the temperature profile alone (with slightly different internal-water parameters).[61] Furthermore, these hydration parameter values are very similar to those obtained for BPTI and mUb (Table 1), which do not cold denature above −35 °C (Figure 2). We therefore conclude that bLg in water at pH 2.6 does not cold denature above −35 °C. This conclusion is apparently at odds with predictions based on calorimetric and CD studies (section S3 of the Supporting Information), but it can be explained by the slow folding kinetics of bLg at low temperatures (Discussion).

To examine bLg under conditions where it is sure to cold denature (on the experimental time scale), we recorded ^{17}O MRD profiles of bLg at pH 2.6 and 4.0 M urea at six temperatures from 19.4 to −30 °C (Figure 5). Under these conditions, bLg is completely dissociated into monomers.[26] According to optical rotation measurements, the cold-denaturation temperature of bLg at pH 3.0 and 4.0 M urea is $T_{cd} = 7$ °C.[26] Differential scanning calorimetry at pH 2.0 and 4.0 M urea yields $T_{cd} = 4$ °C on cooling and $T_{cd} = 13$ °C on heating at a scan rate of 1 K min^{-1}.[29] Our sample should thus be fully native at 19.4 °C and fully cold-denatured at subzero temperatures.

In the global fit to the six MRD profiles (47 data points), we freeze E_{HN}^{-} to the same value as that in the absence of urea. This simplification is justified by the neglible effect of urea on water dynamics in its hydration shell ($\xi_H = 1.00 \pm 0.02$).[76] Furthermore, because the transition width cannot be determined from the fit with useful accuracy, we fix it to a value, $\Delta T_{cd} =$

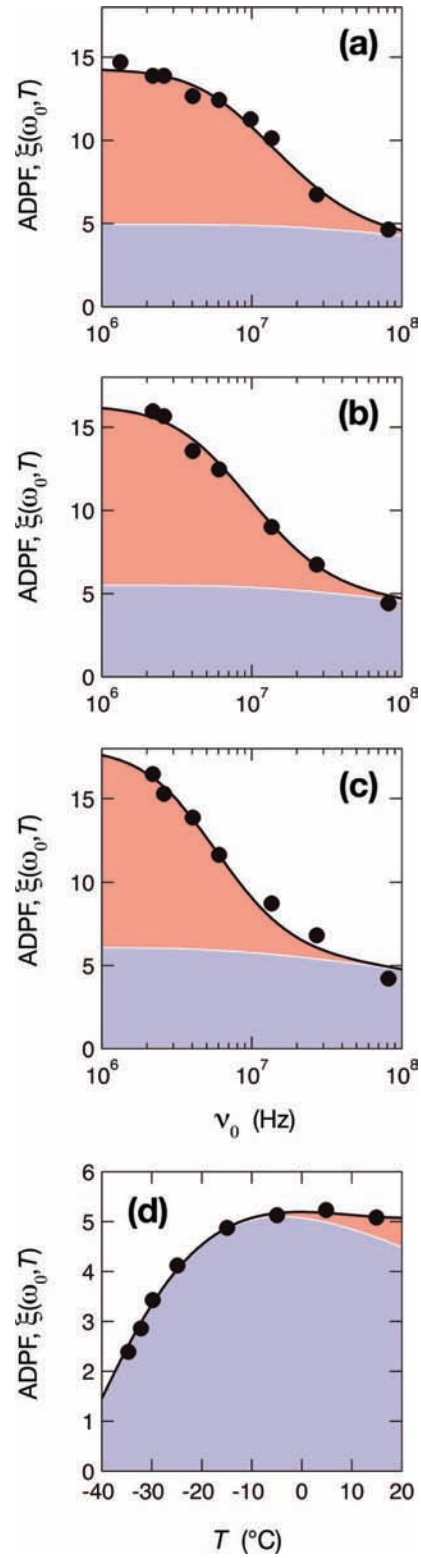

Figure 4. Variation of the water−^{17}O ADPF for bLg at pH 2.6 with frequency (sample 5) at (a) 19.4 °C, (b) 10.2 °C, (c) −1.1 °C, and (d) with temperature (sample 7) at 81.3 MHz. The solid curves were obtained from a global fit to all data (filled circles), including MRD data at −20 and −25 °C (sample 6, Table S1 of the Supporting Information). The resulting parameter values are given in Table 1. The computed ADPF contributions from internal (red) and hydration (blue) water are indicated.

(74) Sakurai, K.; Oobatake, M.; Goto, Y. *Protein Sci.* **2001**, *10*, 2325–2335.
(75) Brownlow, S.; Cabral, J. H. M.; Cooper, R.; Flower, D. R.; Yewdall, S. J.; Polikarpov, I.; North, A. C. T.; Sawyer, D. W. *Structure* **1997**, *5*, 481–495.

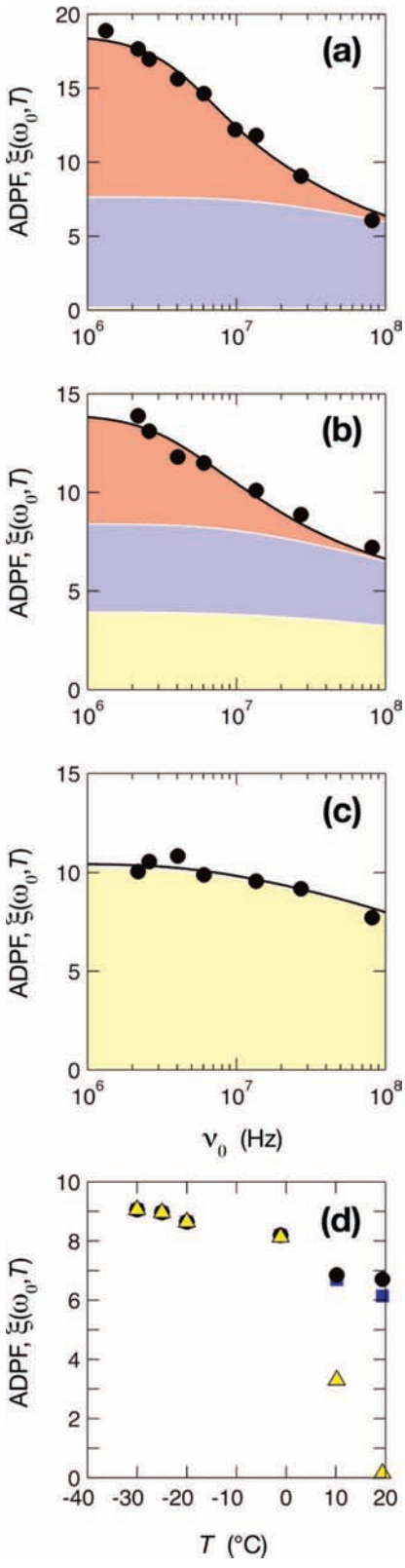

Figure 5. Variation of the water−^{17}O ADPF for bLg at pH 2.6 and 4.0 M urea with frequency (sample 8) at (a) 19.4 °C, (b) 10.2 °C, (c) −1.1 °C, and (d) with temperature at 81.3 MHz. The temperature profile was reconstructed from the MRD profiles in (a)−(c) and at −20, −25, and −30 °C (sample 9). The solid curves were obtained from a global fit to all 6 MRD profiles. The resulting parameter values are given in Table 1. The computed ADPF contributions from internal water (red) and N-state (blue) or D-state (yellow) hydration water are indicated. In panel (d), the contributions from D-state hydration water (yellow triangles) and N- plus D-state hydration water (blue squares) are also indicated.

10 °C, consistent with the calorimetric cold-denaturation enthalpy (cf. eq S7 of the Supporting Information).[29] The data and fitted curves are shown in Figure 5 for the three highest temperatures, which span the cold-denaturation transition. The MRD profiles at the three lowest temperatures closely resemble the one at −1.1 °C, but the ADPF increases slightly with decreasing temperature. This trend is evident in part d of Figure 5, where we have reconstructed the temperature profile from the six fitted ADPF values at 81.3 MHz. (We use fitted values because the highest measurement frequency was 67.8 MHz at the 3 lowest temperatures.)

Unlike all other temperature profiles reported here, the one in part d of Figure 5 does not show the ADPF dropping sharply at low temperatures. The drastic reduction of the ADPF seen in the other cases at temperatures around −30 °C is produced by the very strong (super-Arrhenius) slowing down of molecular rotation (and, hence, of R_1^0) in bulk water at these temperatures.[77,78] In 4 M urea, R_1^0 has a weaker temperature dependence, thereby shifting the drop in the ADPF to attainably low temperatures. In the analysis of the ^{17}O relaxation data, we have taken into account the (modest) increases in solvent viscosity produced by the urea cosolvent (section S1 of the Supporting Information). Furthermore, we use the solvent-exchange model[79,80] to describe the preferential solvation of the protein by urea (section S4 of the Supporting Information).

The ADPF data demonstrate a gradual loss of the internal-water contribution between 19.4 and −1.1 °C (parts a−c of Figure 5), as expected if the protein unfolds on cooling. In contrast, in the absence of urea, the internal-water contribution is fully retained at −1.1 °C (parts a−c of Figure 4) (and at lower temperatures). The global fit in Figure 5 yields $T_{cd} = 10.0 \pm 0.3$ °C, in excellent agreement with previous spectroscopic[26] and calorimetric[29,30] results (Discussion). The exponents $\nu_N = 2.07$ and $\nu_D = 2.21$ differ little from the value 2.17 obtained in the absence of urea, indicating that the fraction hydration water molecules with relatively long correlation times is similar in the three cases. The result $N_{HD}/N_{HN} = 1.3 \pm 0.1$ means that the number of water molecules interacting directly with the protein is 30% larger (675 versus 525) in the cold-denatured state than in the native state in the presence of 4 M urea. The increase in solvent-accessible area will be larger than 30% if the D state has a higher urea affinity than the N state or if water molecules interact simultaneously with different parts of the polypeptide chain (solvation layer overlap).

3.6. *β*-Lactoglobulin at pH 7.2. The native conformation of bLg is more stable at pH 2−3 than at neutral pH. For example, the urea denaturation midpoint concentration at 20 °C is 4.7 M at pH 3.0 but only 4.1 M at pH 7.0,[81] and the cold-denaturation temperature T_{cd} in the presence of 4 M urea increases from 7 °C at pH 3.0[26] to 25 °C at pH 7.0.[36] A (rather long) linear extrapolation from the range 3−5 M urea led to the prediction that $T_{cd} = -14$ °C in the absence of urea at pH 7.0.[36] It therefore seemed likely that cold denaturation of bLg at pH 7 should be observable with the emulsion technique used here.The unusual pH dependence of bLg stability is all the more remarkable

(76) Shimizu, A.; Fumino, K.; Yukiyasu, K.; Taniguchi, Y. *J. Mol. Liq.* **2000**, *85*, 269–278.
(77) Hindman, J. C. *J. Chem. Phys.* **1974**, *60*, 4488–4496.
(78) Lang, E. W.; Lüdemann, H.-D. *Angew. Chem., Int. Ed.* **1982**, *21*, 315–329.
(79) Schellman, J. A. *Biophys. Chem.* **1990**, *37*, 121–140.
(80) Schellman, J. A. *Biopolymers* **1994**, *34*, 1015–1026.
(81) Yagi, M.; Sakurai, K.; Kalidas, C.; Batt, C. A.; Goto, Y. *J. Biol. Chem.* **2003**, *278*, 47009–47015.

because bLg is stabilized by dimer formation at neutral pH. On the basis of reported dimer association constants,[82,83] we expect that 90−95% of the protein in our samples 10−12 exists in dimeric form. Hydrophobically stabilized protein oligomers should dissociate on cooling for the same reason that proteins unfold at low temperatures. However, the small dimer interface in bLg is predominantly polar, and studies by isothermal titration calorimetry indicate that the dimerization constant *increases* slightly on cooling, at least down to 15 °C.[83] The dimerization enthalpy may become positive at lower temperatures, but the available data suggest that the dimer fraction in our samples is unlikely to vary by more than a few percent in the investigated temperature range.

The global fit comprises 82 data points (Figure 6), including MRD profiles at 27, 2, −5, −15, and −25 °C and a temperature profile at 81.3 MHz. (The shape of the 2 and −15 °C profiles, which are not displayed in Figure 6, are intermediate between the ones shown and the fit quality is similar.) In contrast to aMb and bLg in 4 M urea, the data in Figure 6 do not provide any qualitative indications of cold denaturation. However, attempts to fit a one-state model (with temperature-independent protein structure) to the data were unsuccessful, producing systematic deviations well outside the experimental uncertainty. Furthermore, a comparison of the bLg data at pH 2.6 (Figure 4) and pH 7.2 (Figure 6) reveals substantial quantitative differences. At the highest examined temperature, the MRD profiles are similar, the main difference stemming from the different correlation times of the two long-lived internal water molecules (section S2 of the Supporting Information). However, at low temperatures, both the low- and high-frequency ADPFs are much larger at neutral pH than at pH 2.6. Thus, at ∼1 MHz and −25 °C, the ADPF is 3 times larger at pH 7.2, and at 81.3 MHz and −35 °C, the ADPF is a factor 1.7 larger at pH 7.2. This large difference in the temperature dependence of hydration dynamics at pH 2.6 and 7.2 cannot be explained by the dimeric state per se (or by dimer dissociation). Rather, it indicates a temperature-dependent variation in protein structure.

As seen from Figure 6, the two-state model accounts well for the rather large data set at pH 7. In the global fit, we fixed E_{HN}^{-} to the value (27.6 kJ mol^{-1}) obtained at pH 2.6. Furthermore, because the parameters E_{HD}^{-} and N_{HD}/N_{HN} turned out to be strongly coupled in the fit, we imposed the physically motivated (section 3.4) constraint $E_{HD}^{-} = E_{HN}^{-}$. Although the data can be described by a two-state model, the parameter values (Table 1) do not suggest a cooperative unfolding transition. The transition temperature, $T_{cd} = -36 \pm 7$ °C, is 22 °C lower than expected from extrapolation of cold denaturation in urea solvent (above). Furthermore, the transition is very broad, $\Delta T_{cd} = 30 \pm 4$ °C, and does not seem to increase the solvent exposure significantly. The D-state exponent, $\nu_D = 1.56 \pm 0.05$, is even lower than for cold-denatured aMb. As for aMb, we can use the N- and D-state exponents to compute the fraction of hydration water molecules with correlation times τ_H longer than 0.1 ns at 20 °C.[61] This fraction increases from 1.8% (or 13 water molecules) for the N state to 10% (or 64 ± 17 water molecules) for the D state. Similarly, we find that the D state contains 16 ± 4 water molecules with $\tau_H > 1$ ns at 20 °C. Taken together, these results suggest that cooling induces not a cooperative unfolding but a more gradual loosening of the structure, with increased solvent penetration without much change in the solvent-accessible surface area.

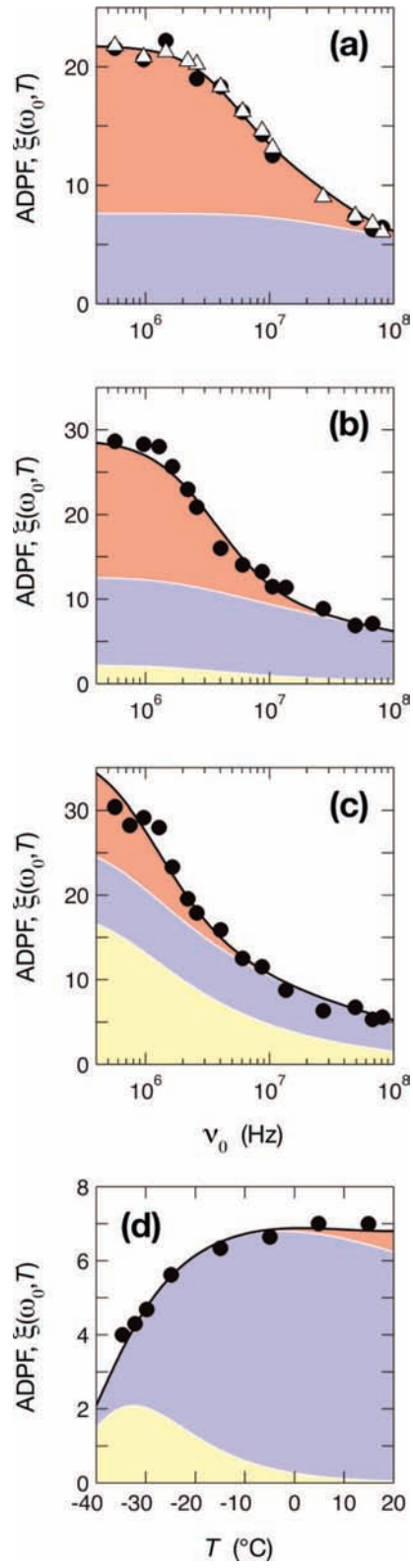

Figure 6. Variation of the water−^{17}O ADPF for bLg at pH 7.2 with frequency (samples 10 −12) at (a) 27 °C, (b) −5 °C, (c) −25 °C, and (d) with temperature (sample 12) at 81.3 MHz. The solid curves were obtained from a global fit to all data (filled circles, emulsion samples; open triangles, solution samples) in panels (a)−(d) plus MRD profiles at 2 and −15 °C. The resulting parameter values are given in Table 1. The computed ADPF contributions from internal water (red) and N-state (blue) or D-state (yellow) hydration water are indicated.

(82) Sakurai, K.; Goto, Y. *J. Biol. Chem.* **2002**, *277*, 25735–25740.
(83) Bello, M.; Pérez-Hernández, G.; Fernández-Velasco, D. A.; Arreguín-Espinosa, R.; García-Hernández, E. *Proteins* **2008**, *70*, 1475–1487.

4. Discussion

4.1. BPTI and Ubiquitin. As long as its three disulfide bonds are intact, BPTI is an exceptionally stable protein with $T_{hd} = 104.5$ °C and $\Delta H_{hd} = 312$ kJ mol^{-1} at pH 4.9.[84] Using these parameters and linear or quadratic fits to the measured[84] temperature dependence of C_p for the N and D states, respectively, we find from the standard two-state thermodynamic relations that BPTI is most stable (maximum N-state population) at −22 °C, where $\Delta G = 50$ kJ mol^{-1}. Further, we obtain a cold-denaturation temperature, T_{cd}, of −112 °C. With water as the solvent, wildtype BPTI is thus not expected to cold denature under any experimentally attainable conditions. Consistent with this prediction, high-resolution ^{1}H NMR spectroscopy indicates that the structure of BPTI (at pH 3.5) is virtually independent of temperature between +30 and −16 °C.[85] Because we can be confident that BPTI remains fully folded at the temperatures examined here (down to −35 °C), the high-frequency temperature profile $R_1(\omega_0,T)$ in part a of Figure 2 reflects the low-temperature hydration behavior of a native protein.

Mammalian ubiquitin lacks disulfide bonds, but the heat-denaturation temperature is still high, $T_{hd} = 90$ °C at pH 4.0.[86] In contrast to BPTI, mUb can be denatured by guanidinium chloride (GdmCl) at 25 °C, with $C_{1/2} = 3.86$ M at pH 4.0 and with little or no residual secondary structure in the D state.[33] Cold denaturation of mUb above 0 °C has been observed in the presence of 3−4 M GdmCl and extrapolation to zero GdmCl concentration yields $T_{cd} = -45$ °C at pH 4.0.[33] Because the stability of mUb increases with pH,[86] T_{cd} should be even lower in our sample at pH 5.0. There are also reports of cold denaturation of mUb at high pressure, $p \geq 2$ kbar.[39,43] A two-state thermodynamic analysis of NMR spectral intensities for mUb at pH 4.5 and 2 kbar yielded $T_{cd} = -12$ °C.[43] At this pressure, the maximum stability of mUb, ΔG (31 °C) = 8.6 kJ mol^{-1}, is only one-third of that at atmospheric pressure. Cold denaturation of mUb at 2 kbar is reported to be highly cooperative, and the D state at −21 °C appears to be almost fully unfolded.[43] It has also been shown that a highly destabilized hydrophobic-core mutant (V26G), with ΔG (25 °C) = 5.9 kJ mol^{-1}, undergoes two-state cold denaturation with $T_{cd} = -12$ °C (at pH 5.9).[87] In summary, these studies show that mUb can undergo cooperative cold denaturation to a highly unfolded state, but only in the presence of an additional, strongly destabilizing perturbation. Under physiological solvent conditions, we expect T_{cd} to be around −50 °C (at pH 5.0). Indeed, high-resolution NMR spectra indicate that the structure of mUb at pH 5.9 is virtually unchanged between +25 and −15 °C.[88] Our finding that mUb remains fully folded at least down to −32 °C is fully consistent with all of the above cited results.

4.2. Cold Denaturation of Ubiquitin in Reverse Micelles. In contrast to our findings, mUb (at pH 5, as in our sample) has been shown by high-resolution NMR spectroscopy to be partly cold-denatured at −20 °C.[89−92] In these studies, temperatures down to −30 °C were accessed without ice formation by encapsulating the protein in reverse micelles, surfactant-covered nanometer-sized water droplets immersed in a nonpolar alkane solvent. The volume of the encapsulated protein−water droplet is some 10 orders of magnitude smaller than the aqueous droplets in our emulsions. Whereas the droplet interface has a negligible effect on our emulsified protein solutions (part a of Figure 3 and part a of Figure 6), the water in reverse micelles is substantially perturbed by the surfactant-covered interface (as well as by the protein). In emulsion droplets, water is in a metastable state at subzero temperatures. This state survives because of the absence of templates for heterogeneous nucleation and because the barrier to homogeneous nucleation is high. In reverse micelles, on the other hand, water remains liquid at subzero temperatures because the equilibrium freezing point is depressed by water−surfactant and water−protein interactions.

In reverse micellar systems, the equilibrium micelle size distribution and the macroscopic phase equilibrium are established by exchange processes involving the transient fusion and fission of the aqueous nanodroplets. If this equilibration process could be arrested, the water in a protein-loaded micelle would probably be unfreezable, forming instead a glass at very low temperatures.[93] So far, the discussion of the possible effects of the reverse micelle on the observed cold denaturation has focused on Coulomb interactions, and it has been shown that modest variations of the net charge of the protein (by pH variation)[89] or of the reverse micelle interface (by varying the surfactant composition)[92] have only minor effects on the cold denaturation of mUb. However, the principal perturbation in a reverse micelle is likely to be a direct consequence of the low water content. Even subtle changes in the thermodynamic properties of the solvent water can have major effects on protein stability.

Under certain conditions, a reverse micelle solution is a thermodynamically stable phase, sometimes called a microemulsion. However, at low temperatures, the microemulsion phase separates into an essentially pure water phase and an alkane-rich phase with dehydrated reverse micelles.[94−98] Low-temperature equilibrium studies are therefore feasible only at low water content, typically less than what is required for the primary hydration shells of the bulky surfactant headgroups and the associated counterions.[99] As a further complication, reverse micelles are dynamic entities that change their size and shape in response to external conditions. Therefore, the usual geometry-based estimate for the size of the (assumed spherical) aqueous core of the reverse micelle is not applicable under the conditions used in cold-denaturation studies. In the absence of protein, the reverse micelles tend to change from spherical to rodlike shape

(84) Makhatadze, G. I.; Kim, K.-S.; Woodward, C.; Privalov, P. L. *Protein Sci.* **1993**, *2*, 2028–2036.
(85) Skalicky, J. J.; Mills, J. L.; Sharma, S.; Szyperski, T. *J. Am. Chem. Soc.* **2001**, *123*, 388–397.
(86) Wintrode, P. L.; Makhatadze, G. I.; Privalov, P. L. *Proteins* **1994**, *18*, 246–253.
(87) Sabelko, J.; Ervin, J.; Gruebele, M. *Proc. Natl. Acad. Sci. U.S.A.* **1999**, *96*, 6031–6036.
(88) Skalicky, J. J.; Sukumaran, D. K.; Mills, J. L.; Szyperski, T. *J. Am. Chem. Soc.* **2000**, *122*, 3230–3231.
(89) Babu, C. R.; Hilser, V. J.; Wand, A. J. *Nat. Struct. Mol. Biol.* **2004**, *4*, 352–357.
(90) Van Horn, W. D.; Simorellis, A. K.; Flynn, P. F. *J. Am. Chem. Soc.* **2005**, *127*, 13553–13560.
(91) Whitten, S. T.; Kurtz, A. J.; Pometun, M. S.; Wand, J. A.; Hilser, V. J. *Biochemistry* **2006**, *45*, 10163–10174.
(92) Pometun, M. S.; Peterson, R. W.; Babu, C. R.; Wand, A. J. *J. Am. Chem. Soc.* **2006**, *128*, 10652–10653.
(93) Gregory, R. B. In *Protein-Solvent Interactions*; Gregory, R. B., Ed.; Marcel Dekker: New York, 1995; pp 191−264.
(94) Zulauf, M.; Eicke, H.-F. *J. Phys. Chem.* **1979**, *83*, 480–486.
(95) Quist, P.-O.; Halle, B. *J. Chem. Soc., Faraday Trans. 1* **1988**, *84*, 1033–1046.
(96) Hauser, H.; Haering, G.; Pande, A.; Luisi, P. L. *J. Phys. Chem.* **1989**, *93*, 7869–7876.
(97) Munson, C. A.; Baker, G. A.; Baker, S. N.; Bright, F. V. *Langmuir* **2004**, *20*, 1551–1557.
(98) Simorellis, A. K.; Van Horn, W. D.; Flynn, P. F. *J. Am. Chem. Soc.* **2006**, *128*, 5082–5090.
(99) Carlström, G.; Halle, B. *Langmuir* **1988**, *4*, 1346–1352.

as they are dehydrated at low temperatures.[95] In the presence of protein, also at room temperature, water is redistributed between droplets that contain protein and those that do not. The amount of water surrounding the encapsulated protein can thus not be estimated from the water/surfactant ratio, as is commonly done.

The marginal stability of native proteins is a result of near cancelation of strong but opposing thermodynamic forces, the largest of which are the conformational entropy of the polypeptide chain and the free energy of hydration of exposed nonpolar side-chains.[10] These two dominant driving forces are both altered by encapsulation of the protein in a reverse micelle. The geometric confinement limits the configurational space available to the polypeptide chain, thereby destabilizing the D state.[100] Limitations in the amount of water and in its configurational freedom (because it is already perturbed by the reverse micelle interface) weaken the hydrophobic effect, thereby stabilizing the D state. Heat-denaturation studies of encapsulated proteins as a function of (total) water content reveal both of these effects and show that the latter is the dominant one at the water contents used in the cold-denaturation studies.[101,102] Moreover, the heat-denaturation enthalpy is substantially reduced in reverse micelles,[101,102] implying that encapsulation makes unfolding less cooperative, as observed for cold denaturation in reverse micelles.[89,91,92]

Reverse micelles have been promoted as a method for studying cold denaturation under native conditions,[89,91,92] without the need for an adjunct perturbation such as urea. In our view, this claim is not justified. Our finding that mUb in supercooled water remains fully folded at least down to −32 °C indicates that the previously reported[89−92] cold denaturation of mUb in reverse micelles is induced by the low water content rather than by the low temperature per se. Our low-temperature results for mUb as well as studies of heat denaturation of other proteins in reverse micelles[101,102] indicate that encapsulation destabilizes the protein substantially. Furthermore, unlike the addition of denaturant, this perturbation cannot easily be extrapolated to zero. (The micrometer-sized emulsion droplets used in our work may be regarded as the limit of negligible solvent perturbation.) If encapsulation in a reverse micelle (of low, but unknown, water content) did not significantly affect the stability of the protein, then also the heat-denaturation temperature, T_{hd}, for the encapsulated protein should be the same as for the protein in aqueous solution. This critical control experiment has apparently not been carried out for mUb. However, for several other proteins, it has been shown that encapsulation can depress T_{hd} by 20−40 °C.[101]

4.3. Apomyoglobin. Circular dichroism studies of equine aMb at pH 5.9 indicate a broad cold-denaturation transition with $\Delta T_{cd} \approx 20$ °C and midpoint $T_{cd} \approx -6$ °C.[49,51] Our ^{17}O MRD data yield a significantly lower cold-denaturation temperature, $T_{cd} = -16 \pm 1$ °C. An acceptable fit to our data cannot be obtained if T_{cd} is fixed to −6 °C. Because a low-temperature baseline was not evident in the CD temperature profiles,[49,51] it is conceivable that a lower T_{cd} would have been obtained had the CD measurements been extended to lower temperatures. Alternatively, the different T_{cd} values deduced from measurements sensitive to secondary structure and hydration may be taken to indicate that cold denaturation of aMb does not occur with full cooperativity, as assumed in the simple two-state model.

What is the structure of cold denatured aMb? If the polypeptide chain were completely unfolded and fully exposed to solvent, we would expect a DPF of ∼2 or less, as for small peptides.[71] However, at temperatures near −30 °C where the D state dominates (part c of Figure 3), the ADPF ξ_{HD} is in the range 4.5−6.0 (eq S12 in the Supporting Information), demonstrating that cold-denatured aMb is far from fully unfolded. Rather, the large ADPF for cold denatured aMb, which is about twice as large as that for native BPTI and mUb at the same temperature (Figure 2), suggests a relatively compact structure penetrated by water molecules (perhaps bridging nearby polypeptide segments) that are more strongly dynamically perturbed than most water molecules in the hydration layer of native proteins. This scenario can account for the broad distribution of hydration water correlation times (as indicated by the small ν_D exponent) for cold denatured aMb, and it is consistent with the indication from CD measurements[51] that the G and H helices are largely intact in cold denatured aMb. Cold denaturation has also been demonstrated for charge-destabilized (low pH) metmyoglobin[45] and apomyoglobin,[47,49] including cold denaturation of the molten−globule intermediate of apoMb.[47,49] The compactness of these cold denatured states depends strongly on pH.[47]

4.4. β-Lactoglobulin in 4 M Urea. Like most other proteins, bLg is unfolded by urea. At 20 °C and pH 3.0, the urea denaturation midpoint concentration, $C_{1/2}$, has been determined to 5.1 M (150 mM ionic strength)[26] or 4.7 M (50 mM ionic strength).[81] At this temperature, $\partial C_{1/2}/\partial T > 0$,[26] implying that the denaturation entropy is negative.[103] Traditionally, the same low-entropy D state is referred to as urea-denatured when it is obtained by increasing the urea concentration and as cold-denatured when it is produced by cooling. At urea concentrations somewhat below $C_{1/2}$, where the protein is highly destabilized but remains predominantly in the native state, further destabilization by cooling can induce unfolding even at ambient temperature. Because of this convenience, cold denaturation of bLg has mostly been studied in the presence of ∼4 M urea.[26,29,30,35,104]

The modest increase of N_H on cold denaturation of bLg in 4 M urea indicates that the D state is not extensively unfolded. This conclusion is consistent with small-angle X-ray scattering (SAXS), CD, and heteronuclear NMR studies, indicating that cold-denatured bLg in 4 M urea at pH 2.5 is relatively compact and exhibits some residual structure, including a native-like β-hairpin stabilized by one of the two disulfide bonds.[35] According to the SAXS measurements, the radius of gyration, R_g, increases by 9% on addition of 4 M urea at 25 °C, by a further 15% on reducing the temperature to 0 °C, and by a further 45% on increasing the urea concentration from 4 to 8 M at 0 °C.[35] The 15% increase of R_g on cold denaturation corresponds to a 52% increase of the effective protein volume, or 11 700 Å^3 of internal solvent. Because the protein is preferentially solvated by urea, the fraction of this volume occupied by urea molecules must be larger than the bulk urea volume fraction at 4 M, which is 18%. We thus estimate that ∼300 water molecules penetrate the denatured protein. This

(100) Zhou, H.-X.; Dill, K. A. *Biochemistry* **2001**, *40*, 11289–11293.
(101) Battistel, E.; Luisi, P. L.; Rialdi, G. *J. Phys. Chem.* **1988**, *92*, 6680–6685.
(102) Shastry, M. C. R.; Eftink, M. R. *Biochemistry* **1996**, *35*, 4094–4101.
(103) Scharnagl, C.; Reif, M.; Friedrich, J. *Biochim. Biophys. Acta* **2005**, *1749*, 187–213.
(104) Nölting, B. *Biochem. Biophys. Res. Commun.* **1996**, *227*, 903–908.

estimate does not clearly distinguish internal from external hydration, but it suggests that the SAXS and MRD results are compatible.

The failure of the two-state model to describe cold denaturation of bLg is clearly indicated by the large difference between the calorimetric and van't Hoff denaturation enthalpies.[29,30] Another observation pointing to a more complex process is the finding that the far-UV ellipticity shows no sign of leveling off even at −10 °C, although, according to the two-state model, the transition should be complete at 0 °C.[35] The gradual loss of residual structure on cooling below the main transition, indicated by the ellipticity data,[35] is likely to be accompanied by a gradual expansion of the, initially rather compact, cold-denatured protein. An increase of N_{HD} as the protein expands on further cooling below T_{cd} can explain the anomalously large apparent activation energy E_{HD}^{-} (Table 1). At high frequencies, the D-state contribution to R_1 is proportional to $N_{HD}\langle\tau_{HD}\rangle$. Even if $\langle\tau_{HD}\rangle$ has the same temperature dependence as $\langle\tau_{HN}\rangle$ (as we expect), a temperature dependence in N_{HD}, if not explicitly accounted for by the model, will give rise to an *apparent* activation energy E_{HD}^{-} that differs from E_{HN}^{-}. The finding that $E_{HD}^{-} > E_{HN}^{-}$ implies that N_{HD} increases on cooling. That the large E_{HD}^{-} is an artifact of imposing the two-state model (with temperature-independent D-state structure) is also suggested by the result of a fit to a restricted data set including only the MRD profiles at the three highest temperatures (the ones shown in Figure 5). In this fit, which is of slightly better quality than the fit to all six profiles, there is no significant difference between E_{HD}^{-} and E_{HN}^{-} (Table 1).

4.5. Kinetics of Cold Denaturation. In analyzing the ^{17}O relaxation data, we have tacitly assumed that the measurements were carried out on samples containing an equilibrium ensemble of protein molecules. We thus assumed that the protein conformations present in the sample are given by the Boltzmann distribution, (eq S5 in the Supporting Information), at each temperature. (Neither the emulsion droplets nor the supercooled water are in thermodynamic equilibrium, but this does not affect the N ⇌ D equilibrium.) However, because the rate of protein unfolding varies strongly with temperature,[105] cold denaturation may be too slow to be observed on the experimental time scale, even though the D state is more stable than the N state. In other words, the protein may be kinetically trapped in the N state at low temperatures. To observe cold denaturation, the sample equilibration time, τ_{eq}, must not be much shorter than the conformational relaxation time, τ_{rlx}, defined as

$$\tau_{rlx}(T) = \frac{1}{k_f(T) + k_u(T)} \qquad (2)$$

where k_f and k_u are the folding and unfolding rate constants (for a two-state protein). For the temperature profiles, the samples were equilibrated 25−30 min at the measurement temperature and kept at 4 °C for at least 2 h between measurements at different temperatures. For the MRD profiles, the samples were maintained at the fixed temperature for several hours while performing relaxation measurements at the lower magnetic fields. Thus, $\tau_{eq} \approx 0.5-3$ h.

The fact that we do observe cold denaturation in the temperature profile of aMb (part c of Figure 3) shows that, at least for this protein, $\tau_{rlx} \ll 1$ h even at −20 °C. This conclusion is consistent with the CD observation of aMb cold denaturation on cooling from +20 to −9 °C at a rate of 0.5 K min^{-1}.[49] The question that we must now address is whether also mUb and bLg, for which we do not observe cold denaturation, would unfold sufficiently rapidly at low temperatures. A quantitative analysis (section S5 of the Supporting Information) indicates that the N state of mUb is *not* kinetically trapped but is actually thermodynamically stable down to −32 °C, whereas bLg may be kinetically trapped in the N state (on our experimental time scale) if $T_{cd} < 0$ °C.

In an attempt to extend the experimental time scale, we measured the water−^{17}O R_1 in emulsion samples (∼1 mM bLg, pH 2.6) that were continuously maintained at different fixed temperatures between 0 and −30 °C. These measurements were performed at a fixed low frequency (2.6 MHz), where unfolding should be manifested as a substantial reduction in R_1 due to the loss of the long-lived internal water molecules. On the basis of these results (section S6 of the Supporting Information), we can conclude that $T_{cd} < -5$ °C for bLg in water at pH 2.6. If T_{cd} were ≥ − 5 °C, we would have seen the cold denaturation. If T_{cd} is lower, bLg will be kinetically trapped in the N state on our experimental time scale. Because dimeric bLg at pH 7.2 is not likely to have drastically faster (un)folding kinetics than the monomer at pH 2.6, we can also conclude that the structural changes indicated at low temperatures (with an apparent T_{cd} of −36 °C) do not correspond to complete cold denaturation.

5. Conclusions

The molecular basis of the generic stability maximum of soluble globular proteins and the associated phenomenon of cold denaturation is not fully understood, but hydration effects are generally thought to play a key role. Yet, changes in protein hydration on cold denaturation have not been investigated experimentally. Here, we have addressed this fundamental issue by using water−^{17}O spin relaxation to monitor the hydration of four proteins from room temperature down to −35 °C. Such low temperatures could be reached without ice formation by containing the protein solution in picoliter emulsion droplets with ∼10^8 protein molecules. Control experiments demonstrated that containment does not influence the system or the measurements. The turbidity and inhomogeneous magnetic susceptibility of emulsions severely limit the number of physical techniques that can be applied to study the contained protein solution. Optical spectroscopy studies of emulsified protein solutions have been reported,[44,59] but it is not clear that the observed changes in UV absorbance reflect cold denaturation rather than subunit dissociation or localized structural changes.

Few, if any, proteins have been shown to cold denature under otherwise native conditions. Although most, or all, proteins are expected, on thermodynamic grounds, to cold denature in water, freezing of the solvent or slow unfolding kinetics usually prevent observation of the transition. In accordance with this experience, none of the three unmodified proteins examined here (BPTI, mUb, and bLg) was found to cold denature in water above −32 °C. For BPTI and mUb, the native state is expected to remain stable down to this temperature, whereas, for bLg, cold denaturation is too slow to be observed on the time scale set by the limited lifetime of the supercooled emulsion droplets. For bLg at pH 2.6, our data indicate that the cold denaturation temperature is lower than −5 °C, which is consistent with the available thermodynamic data on this protein.[29,30] For dimeric bLg at pH 7.2, we infer hydration changes with a likely structural origin, but they are not characteristic of cold denaturation. Our finding that mUb remains folded down to −32

(105) Bachmann, A.; Kiefhaber, T. In *Protein Folding Handbook*; Buchner, J., Kiefhaber, T., Eds.; Wiley-VCH: Weinheim, 2005; Vol. I, pp 379−410.

°C is consistent with a cold-denaturation temperature of −45 °C, as predicted by extrapolation of data on the urea-assisted cold denaturation of mUb.[33] Furthermore, our results suggest that the cold denaturation observed at −20 °C for mUb encapsulated in reverse micelles[89−92] is induced by the low water content rather than by the low temperature per se. The one protein for which we did observe cold denaturation in water is apomyoglobin, which is destabilized by heme removal. Our ability to directly monitor hydration changes and to access lower temperatures than hitherto[49,51] indicates that cold denaturation of aMb is not a simple two-state transition.

As expected from previous studies,[26,29,30,35] we find that bLg cold denatures at 10 °C in 4 M urea. Our data indicate that the cold-denatured protein is relatively compact, in agreement with SAXS data,[35] and that it expands on further cooling. For both bLg and aMb, the cold-denatured protein is thus better described as solvent-penetrated than as unfolded. If this turns out to be a general feature of cold-denatured proteins, then the widely accepted analogy between cold denaturation and the aqueous solubility of small nonpolar molecules is misleading. This conclusion follows because water penetration of the hydrophobic core and transfer of nonpolar side-chains into water have opposite thermodynamic signatures: low temperature facilitates transfer of nonpolar molecules into water but not transfer of water into nonpolar media.[106]

The results presented here and elsewhere[61,71] show that the hydration layer of native proteins, with the exception of a small fraction of secluded hydration sites, is indistinguishable form the hydration shell of a small organic solute. In contrast, even an extensively unfolded, random-coil-like protein is expected to be hydrated in an essentially different way from a fully extended polypeptide chain or a solution of small molecules. Even a random-coil-like protein is likely to contain regions where water molecules bridge polypeptide segments with strong conformational preferences and relatively slow dynamics. The more compact cold-denatured state may contain strings and sheets of water molecules embedded in, and interacting strongly with, the disordered protein. The thermodynamic and kinetic properties of such water molecules are likely to differ substantially from those of water in the hydration shell of a small molecule surrounded by bulk water.

The view outlined here is opposite to the conventional one, where the native protein has unusual hydration properties and the denatured protein is hydrated like a collection of small molecules. So far, theoretical studies of the mechanism of cold denaturation have either used oversimplified models,[14,16,18,19,21] treated the D state as fully solvent-exposed,[15,17] or considered only the N state.[22] It seems clear, however, that a full understanding of cold denaturation will require further experimental characterization of the structure and hydration of cold-denatured proteins.

Acknowledgment. We thank Hans Lilja for spectrometer maintenance, Hanna Nilsson for protein purification, and Erik Persson for helpful advice and discussions. This work was supported by the Swedish Research Council, the Knut & Alice Wallenberg Foundation, and the Wenner-Gren Center Foundation for Scientific Research.

Supporting Information Available: Spin relaxation data, equations, and figures; table of samples investigated by ^{17}O MRD. This material is available free of charge via the Internet at http://pubs.acs.org.

JA8056419

(106) Goldman, S. *Can. J. Chem.* **1974**, *52*, 1668–1680.